

Multi-toric optical element to compensate ocular astigmatism with increased tolerance under rotation

DIANA GARGALLO^{1*}, ANABEL MARTINEZ- ESPERT², SARA PERCHES¹, M. VICTORIA COLLADOS¹, LAURA REMÓN¹, JORGE ARES¹

¹ Applied Physics, University of Zaragoza, Zaragoza, Spain.

² Departamento de Óptica y Optometría y Ciencias de la Visión, Universitat de València, Burjassot, Spain.

*dqarqallo@unizar.es

Received 16 January 2024; revised 15 March 2024; accepted 18 March 2024; posted 20 March 2024; published 17 April 2024

A new, to the best of our knowledge, optical element designed to compensate regular astigmatism while exhibiting increased tolerance to rotational misalignment is introduced. The element incorporates an optical design based on concentric annular regions with slightly different cylindrical axis angular positions. To assess visual quality performance as a function of rotation, retinal image simulation and clinical assessments with an adaptive optics visual simulator were carried out. The results demonstrate the superior performance of the newly proposed element in the presence of rotational errors when compared to traditional solutions. ©2024 Optica Publishing Group <https://doi.org/10.1364/OL.518973>

Healthy human eyes do not always achieve optimal vision quality due to refractive errors as myopia, hyperopia, regular and irregular astigmatism. In the case of regular astigmatism, optimal visual acuity (VA) can be got through lenses with spherocylindrical (S-C) power caused by toric surfaces. However, it is important to note that to achieve the corresponding compensatory effect, the astigmatic lens must be carefully oriented in the plane transverse to the visual axis. When a lens S-C power is not well aligned with the astigmatism axis of refractive error of the eye, the lens may induce higher astigmatic vision degradation instead of achieving optimal compensation [1,2]. Keeping the correct rotational position of a lens to compensate astigmatism pose different challenge levels depending on whether they are used as eyeglasses, contact lenses or intraocular lenses. Among all of them, due to its dynamic condition, contact lenses present the most challenging case.

There are several factors involved in rotational stability of a S-C contact lens. The patient related factors include palpebral aperture, lid position and corneal topography [3]. The factors related to the contact lens include fitting profile, lens movement after blinking, mechanical properties of the material (e.g. Young modulus) and toric lens stabilization design. Nowadays, various stabilization techniques are used in S-C contact lenses, such as prism ballast, periballast or dynamic stabilization, which are surfaced on the contact lens [4-6]. However, this kind of methods also increase the complexity of the lens design and may also cause discomfort due to the added thickness at the lens periphery required to implement the stabilization structures. Nevertheless, a maximum angular

misalignment of 6.00° can still easily occur due to blinking interaction with the lens in the primary sight position [7].

In this work, a new kind of optical design to compensate astigmatism has been developed accepting that a contact lens may not always be well aligned with the astigmatism axis. The idea keeps a close analogy relation with the multifocal contact lens designs used to compensate presbyopia by simultaneous vision [8,9].

In particular, it is purposed a multizonal toric design of the optical region for the contact lens formed by a set of annular concentric regions. In its most straightforward version, all the zones have the same S-C power with slightly different cylindrical axis angular positions. In this way, it is expected that at least one of the zones correct the astigmatism when the lens rotates due to blinking interaction.

This new optical multizonal design zone may be surfaced onto the optical zone of the contact lens body and can also exist together with the current position stabilization methods. The optical design implies a new element able to tolerate higher degrees of angular rotation errors, this characteristic implies an increased quality visual stability and/or the use of less demanding and comfortable stabilizations methods.

Figure 1 illustrates the new proposed element in a trizonal setting (Figure 1(b) in comparison with a conventional S-C lens (Figure 1(a)). The design can be potentially customized in function of the specific magnitude of astigmatism, blur tolerance and pupil size of each patient.

For this study, the design was set with a 5.00° rotation, and a maximum optical zone diameter of 4.50 mm. The central zone has a radius of 1.40 mm, the mid-peripheral zone has a radius of 1.87 mm, and the peripheral zone has a radius of 2.25 mm. In terms of S-C power, the most peripheral zone presents the S-C zero-misaligned nominal prescription (S-C_{N0}), the mid-peripheral zone presents the same S-C power with a clockwise (CW) - 5.00° rotated position for the cylinder axis (S-C_{CW5}) and the central zone has a counterclockwise (CCW) + 5.00° rotated position (S-C_{CCW5}). It has been established that counterclockwise is considered positive, while clockwise is considered negative.

To evaluate the performance of this new optical element in the presence of a rotational error, simulated retinal images and clinical evaluations were done for the compensation of an astigmatic ametropia of -3.50 D × 180°.

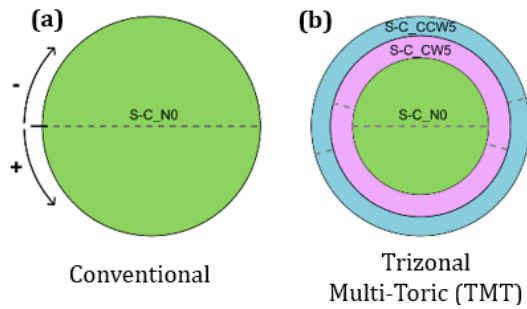


Fig. 1. Different designs of tested optical zones. (a) Conventional spherocylindrical (S-C) contact lens. (b) Trizonal Multi-Toric (TMT) design. The green ring denotes the S-C prescription with correct axis of astigmatism (S-C_{N0}). The purple ring denotes the 5.00° S-C prescription rotated clockwise for the cylinder axis (S-C_{CW5}). The blue ring denotes the 5.00° S-C prescription rotated counterclockwise for the cylinder axis (S-C_{CCW5}). The dashed line indicates the direction of the negative cylinder axis.

On the one hand, the retinal image simulations illustrate how a line of optotypes corresponding with 0 LogMAR visual acuity (5' arc of angular size) can be seen with the new multi-toric design in comparison with a conventional toric compensation (see Figure 2). The retinal image calculation was done as the convolution of the paraxial image with the point-spread function (PSF), calculated using the Fourier optics method [10] by Matlab v.7 (The Mathworks Inc., Natick, MA, USA) for a reduced eye model with aperture radius 2.250 mm, refractive index 1.333 and axial length 22.222 mm. The effect of the astigmatic wavefront aberration of the eye in combination with each compensation element were modeled as a thin phase plate at the aperture plane of the model eye. The compensations were then rotated in increments of $\pm 2.50^\circ$, ranging from 7.50° (counterclockwise) to -7.50° (clockwise) relative to the nominal position. The optical zone's aperture was set to the same 2.25 mm radius as the eye model.

In the case of the conventional S-C design (see Figure 2), it is evident that image quality declines as rotation error increases, transitioning from very good to unacceptable image quality at $\pm 5.00^\circ$ of rotation error. In contrast, the new multi-toric design the optical shows enhanced tolerance to rotation error in terms of potential visual acuity.

On the other hand, a double-blind clinical study was performed. Inclusion criteria consisted of healthy individuals who had not undergone refractive surgery, were not taking medications affecting vision or the eye, were aged between 18 to 35 years, spherical refractive error less than 4.00 D of myopia or hyperopia, and astigmatism refractive error less than 1.00 D. The contact lens users discontinued their use 48 hours before the measurements. The study adhered to the principles in the Helsinki Declaration and every participant provided written informed consent.

The clinical evaluation was carried out with the adaptive optics visual simulator (VAO, Voptica SL, Murcia, Spain). This commercially available device combines a Hartmann-Shack sensor to measure the objective refraction and wavefront aberrations of the eye, and a silicon liquid crystal spatial light modulator (LCoS) that allows for compensation of ocular refraction and aberrations, as well as the simulation of different optical profiles [11-14].

Refraction was measured three times with the Hartmann-Shack sensor to obtain an average, which served as the initial reference for the subjective refraction process. Compensation for each patient's

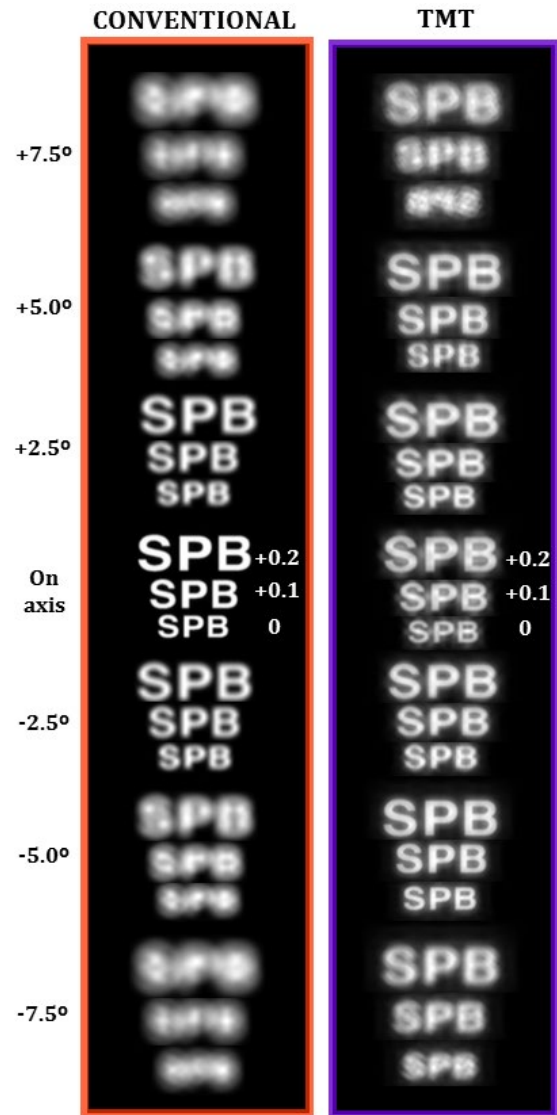


Fig. 2. Simulated multi-line images corresponding with LogMar VA = (0.0, +0.1, +0.2) for different rotation errors in a model eye with spherocylindrical refraction ($-3.50 \text{ D} \times 180^\circ$). On the left, the simulation for a conventional spherocylindrical compensation, on the right the corresponding simulation for the trizonal multi-toric (TMT) design.

refraction, induction astigmatic ametropia ($-3.50 \text{ D} \times 180^\circ$), and conventional or multi-toric design (See Figure 1) of the lenses with different rotations were all performed simultaneously thanks to LCoS the phase spatial modulator provided by the instrument.

For the sake of completeness, rotation was carried out both clockwise (negative) and counterclockwise (positive) at 2.50° , 5.00° , and 7.50° in both directions. For each design and condition, VA was measured using the Snellen E optotype, which displayed 5 random letters per line with + 0.10 logMAR steps between lines, down to -0.2 logMAR , using the OLED display integrated within the instrument. To assess the VA of each patient with different designs, participants were instructed to identify the optotypes of each line from left to right and from lower to higher VA. The last line of VA they could correctly recognize was documented, and errors in letter identification were discounted (assigning each letter a value of +

0.02 logMAR). The optotype was projected to infinity with an average photopic luminance of 80 cd/m². The different lenses and orientations were randomly presented to the patient.

Throughout the study, changes in the pupil diameter of the patients were monitored, revealing an average diameter of 6.96 ± 1.04 mm. However, the assessment of visual performance was carried out with a fixed pupillary diameter of 4.50 mm, as this dimension represents the inherent limitation of the visual simulation instrument. No participant exhibited a measurement below this value. All measurements were carried out randomized order in a single session, which took 45 to 60 minutes to complete. Throughout the entire process of recording measurements, neither the examiner nor the patient knew which optical element was being evaluated.

Descriptive statistics were used to describe the data and the normality of data was assessed with the Shapiro–Wilk test which indicated normal distribution. The paired t-Test was used to statistical analysis. In all tests, the significance level was considered 0.05. Regression fitting and the correlation coefficient (r²) were obtained to analyze the relationship between the loss of VA and the degree of rotation.

The study included 16 eyes of 16 volunteers (62.5 % OD and 37.5 % OS), 15 were women and 1 was a man. The mean age was 22.75 ± 3.29 years (range 19 to 32 years). Regarding the subjective refractive error, the mean sphere (sph) was -1.39 ± 1.30 D (range 0 to -3.50 D), while the mean cylinder (cyl) was -0.20 ± 0.30 D (range 0 to -0.75 D). The sph and cyl values used for averaging were taken from the spherocylindrical refractions expressed in minus cylinder form. The mean of the best corrected distance VA was -0.08 ± 0.05 logMAR (range -0.18 to + 0.0 logMAR). Mean higher-order Zernike Root Mean Square (RMS) for a pupil diameter of 4.50 mm was 0.14 ± 0.06 μm.

First, we compared the VA achieved with clockwise rotation to that obtained with counterclockwise rotation for each considered design. Figure 3 shows box plots of VA for all data samples for different lenses (conventional and TMT) and all considered rotations: on-axis (a), ± 2.50° (b), ± 5.00° (c) and ± 7.50° (d). For the same rotation value within a given design, no statistically significant differences were found between both directions: conventional toric (p= 0.05) and TMT (p= 0.125).

Table 1 summarizes the mean and standard deviation (SD) of VA data for each element and rotation (averaging between clockwise and counterclockwise rotations was considered). The bottom line shows the polynomial regressions for the Visual Acuity as a function of the rotation error together with Pearson's correlation coefficient for both studied cases.

Table 2 displays the experimental differences in VA between each rotation and the on-axis position for every optical element. Statistically significant differences were observed for the conventional design in VA between the on-axis position and each rotation; in particular, there was a loss of two lines in VA at 7.50° of rotation error.

Our results show that with the nominal compensation position, VA is better with the conventional toric design compared to the TMT design (statistically significant difference, p<0.05). However, once the rotation occurs, the average VA with the conventional design decreased from - 0.07 on-axis to + 0.13 at 7.50° of rotation error. In contrast, for the TMT design, VA mean goes from +0.01 on-axis to +0.07 with a rotation error of 7.50°. The differences at the

most extremal rotated position were statistically significant for both designs (p<0.05).

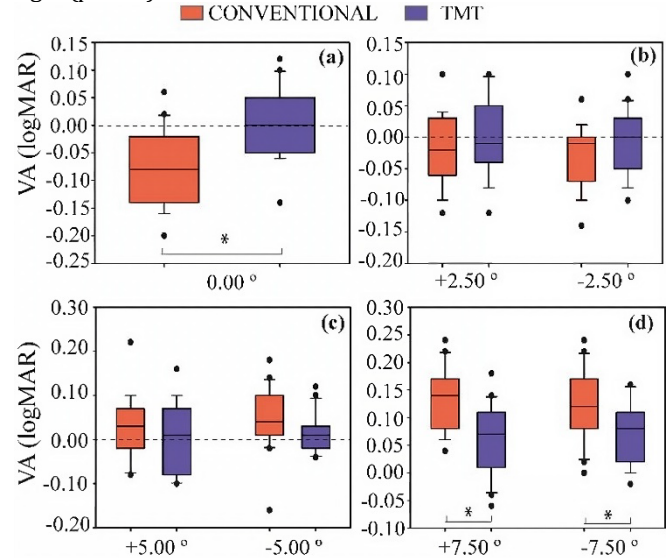


Fig. 3. Box plots of VA for all data samples for different lenses and all rotations: (a) on-axis, (b) ± 2.50°, (c) ± 5.00° and (d) ± 7.50°. The median (central line inside each box), Q1 and Q4 quartiles (lower and higher borders of each box, respectively), and maximum and minimum values (whiskers) are shown for each box. * Significant pairwise differences.

Table 1. Visual acuity (mean ± SD) for all for each design and rotation. In the last line (grey background) it is shown the regression fitting and the r² as a function of the rotation.

Rot	Visual Acuity (logMAR)			
	Conventional		TMT	
	Experiment	Fig.2	Experiment	Fig.2
On-axis	- 0.07 ± 0.07	≤ 0	+ 0.01 ± 0.07	≤ 0
[2.50°]	- 0.02 ± 0.04	≤ 0	+ 0.00 ± 0.05	≤ 0
[5.00°]	+ 0.05 ± 0.05	+ 0.20	+ 0.02 ± 0.05	≤ 0
[7.50°]	+ 0.13 ± 0.05	≥+ 0.20	+ 0.07 ± 0.06	+ 0.15
VA =	0.03 Rot-0.085		0.0024 Rot ² -0.01	
r²	0.99		1.00	

*For each rotation, averaging between clockwise and counterclockwise rotations was taken into account. Rot: Rotation error. The columns labelled as "Fig.2" represent VA values estimated from the simulated multi-line images shown at Fig.2. In the last line (grey background), the regression fitting and the r² as a function of the rotation are shown

Table 2. Visual acuity and t-test differences to evaluate between rotations for the same element.

Rot	VA Differences (logMAR) and p-value On-axis			
	Conventional		TMT	
[2.50°]	+ 0.05	p< 0.002*	- 0.01	p= 0.620
[5.00°]	+ 0.12	p<0.001*	+ 0.01	p= 0.551
[7.50°]	+ 0.20	p<0.001*	+ 0.06	p= 0.005*

* Statistically significant differences (p<0.05). Rot: Rotation error.

Conversely, the new elements showed increased tolerance to rotation error (see Table 1 and Figure 3). For the TMT design, statistically significant differences were only found between the centred and maximum rotation positions (Table 2). In the TMT design, there was a loss of 3 letters in VA (+ 0.06 logMAR), and in the conventional design there was a loss of 10 letters in VA (+ 0.20 logMAR).

Table 1 also reveals that the average values of experimental visual acuity exceed those estimated from the simulated images shown in Fig. 2. This finding is more evident in cases with larger rotational errors. Among other causes, the reasons for these differences may be attributed to the limitations of the reduced eye model or to perceptual adaptation to astigmatic image degradation [15,16].

In the case of the conventional S-C design, there is a noticeable decrease in simulated image quality as the rotation error increases. This is reflected in clinical outcomes, where VA shifts from being very good with the centered design (- 0.07 logMAR) to deteriorating significantly with a 7.50 ° rotation (+ 0.13 logMAR) (Table 1). In contrast, the TMT design show greater tolerance to rotation error. As can be seen in Figure 2 and in clinical results (Table 1 and Figure 3), image quality remains quite stable across all angular errors, even up to a 7.50 ° rotation.

Regarding the limitations of the study with patients, the adaptation time to each optical element and condition was short, a different study must be performed to determine if this condition can influence the obtained results. Moreover, only one pupil size and optotype contrast has been considered in the clinical study, In the future, it might be of interest to evaluate the performance of the new element using different pupil diameters and optotypes with reduced contrasts.

Results may have important implications in the management of astigmatism correction because it is expected that the stable image quality of the new proposed under rotation implies better visual comfortability for toric contact lenses users. From a clinical viewpoint, the proposed multitoric design might be helpful for subjects with large amount of manifest cylinder who have experienced previous unsuccessful fittings of toric contact lenses. However, due to the inverse relationship between visual quality tolerance to rotation and cylinder power [1], fewer VA gains should be expected for astigmatism cylinder powers lower than 3.50 D, as analyzed in this study. Since low astigmatism powers are more prevalent [17], the clinical application of this design for the general population deserves further research.

Moreover, contact lenses manufacturers can also be benefited for the increased rotation tolerance of these designs because smaller stock range will be needed for different cylinder axis. Fabrication of TMT design implies toric surfacing so, a priori, can be fabricated with lathe cutting machine with a special program setting. Nevertheless, further research needs to be conducted to manufacture and testing this new type of contact lenses for astigmatism compensation.

In summary, we have introduced a new optical design capable of compensating for regular astigmatism with increased tolerance to rotation error. Several retinal image simulations have shown that these new designs provide acceptable and quite stable retinal image quality compared with conventional design when the lens rotates a range of 7.50°. These results have been corroborated by a double-blind clinical study with the help of a commercial visual simulator based on adaptive optics. Taking all this together, it seems that the proposed multi-toric designs present an interesting alternative solution to compensate regular astigmatism with increased tolerance to rotational misalignment errors.

Funding. This research was supported by Ministerio de Ciencia, Innovación y Universidades (Grant PID2020-114311RA-I00) and Gobierno de Aragón (Grant E44-23R). D. G. Y. was supported by Gobierno de Aragón.

Acknowledgments. A. M-E. acknowledges financial support from Ministerio de Ciencias e Innovación (Grant PID2022- 142407NB-

100), Generalitat Valenciana (Grant CIPROM/2022/30), and Universitat de València (programa Atracció de Talent 2021).

Disclosures. The authors declare no conflicts of interest.

Data availability. Data underlying the results presented in this paper are not publicly available at this time but may be obtained from the authors upon reasonable request.

References

1. S. A. Read, S. J. Vincent and M. J. Collins, "The visual and functional impacts of astigmatism and its clinical management," *Ophthalmic Physiol. Opt.* **34**, 267–294 (2014).
2. J. S. Wolffsohn, G. Bhogal and S. Shah, "Effect of uncorrected astigmatism on vision," *Journal of Cataract & Refractive Surgery* **37**, 454-460 (2011).
3. G. Young, C. Hunt, M. Covey, "Clinical evaluation of factors influencing toric soft contact lens fit," *Optom Vis Sci* **79**,11-9 (2002).
4. M. G. Harris, M. R. Decker, Funnell, J. W, "Rotation of spherical nonprism and prism-ballast hydrogel contact lenses on toric corneas," *American Journal of Optometry and Physiological Optics* **54**(3), 149-152 (1977).
5. A. J. Phillips and L. Speedwell, (No Title). Contact lenses (2007).
6. A. J. Hanks, "The watermelon seed principle". In *Contact Lens Forum* (Vol. 8, No. 9, 61-70)(1983).
7. A. Tomlinson, W. H. Ridder III, and R. Watanabe, "Blink induced variations in visual performance with toric soft contact lenses," *Optom. Vision Sci.* **71**, 545-549 (1994).
8. J. Ares, R. Flores, S. Bará, *et al.*, "Presbyopia compensation with a quartic axicon," *Optom Vis Sci.* **82**, 1071-1078 (2005).
9. J. Ares, S. Bará, M. Gomez, *et al.*, "Imaging with extended focal depth by means of the refractive light sword optical element," *Opt. Express* **16**, 18371-18378 (2008).
10. S. Perches, M.V. Collados and J. Ares, "Retinal Image Simulation of Subjective Refraction Techniques," *PLoS ONE* **11**, e0150204 (2016).
11. P.A. Piers, E.J. Fernandez, S. Manzanera, *et al.*, "Adaptive optics simulation of intraocular lenses with modified spherical aberration," *Investig. Ophthalmol. Vis. Sci.* **45**, 4601-4610 (2004).
12. E.J. Fernández, S. Manzanera, P. Piers, *et al.*, "Adaptive optics visual simulator," *J. Refract. Surg.* **18**, 634-638 (2002).
13. J. Tabernerero, C. Otero and S.A. Pardhan, "Comparison between refraction from an adaptive optics visual simulator and clinical refractions," *Transl. Vis. Sci. Technol.* **9**, 22 (2020).
14. L. Hervella, E.A. Villegas, C. Robles, *et al.*, "Spherical aberration customization to extend the depth of focus with a clinical adaptive optics visual simulator," *J. Refract. Surg.* **36**, 223-229 (2020).
15. L. Remón, J. A. Monsoriu and W. D. Furlan, "Influence of different types of astigmatism on visual acuity," *J. Optom.* **10**, no. 3, 141-148 (2017).
16. M. Vinas, P. de Gracia, C. Dorransoro, *et al.*, "Astigmatism impact on visual performance: meridional and adaptational effects," *Optom Vis Sci.* **90**, 1430-1442 (2013).
17. P.G. Sanfilippo, S. Yazar, L. Kearns, *et al.*, "Distribution of astigmatism as a function of age in an Australian population," *Acta Ophthalmol.* **93**, e377- e385 (2015).